Applied Catalysis B: Environmental 140–141 (2013) 619–625

Contents lists available at SciVerse ScienceDirect

Applied Catalysis B: Environmental

journal homepage: www.elsevier.com/locate/apcatb

Photocatalytic oxidation of nitrogen oxides on N-F-doped titania thin films

Antigoni V. Katsanaki [a,c], Athanassios G. Kontos [a,*], Thomas Maggos [b], Miguel Pelaez [d], Vlassis Likodimos [a], Evangelia A. Pavlatou [c], Dionysios D. Dionysiou [d], Polycarpos Falaras [a,*]

[a] Division of Physical Chemistry, Institute of Advanced Materials, Physicochemical Processes, Nanotechnology and Microsystems (IAMPPNM), National Center for Scientific Research "Demokritos", 153 10 Aghia Paraskevi Attikis, Athens, Greece
[b] Institute of Nuclear Technology - Radiation Protection, NCSR 'Demokritos' Aghia Paraskevi Attikis, 15310, Athens, Greece
[c] General Chemistry Laboratory, School of Chemical Engineering, National Technical University of Athens, 9 Heroon Polytechniou Str, Zografou 15780, Athens, Greece
[d] Environmental Engineering and Science Program, University of Cincinnati, Cincinnati, Ohio 45221-0012, USA

ARTICLE INFO

Article history:
Received 25 January 2013
Received in revised form 23 April 2013
Accepted 30 April 2013
Available online 8 May 2013

Keywords:
Air treatment
Continuous flow reactor
Nitrogen-Fluorine doped TiO_2
Daylight photocatalysis

ABSTRACT

Visible light activated nanostructured TiO_2 with nitrogen and fluorine co-dopants were prepared by the surfactant assisted sol–gel method and immobilized on glass substrates by dip coating. The films were inserted inside a continuous flow photoreactor and examined for the photocatalytic oxidation of NO air pollutant with initial concentration of 200–800 ppbv. The modified catalysts exhibited significant photocatalytic activity under daylight illumination, with maximum percentage of NO removal equal to 24.2% and photooxidation rate up to 0.66 $\mu g\,m^{-2}\,s^{-1}$. The reaction rates increased proportionally to the incident light intensity whereas for the strongly absorbed UV light a deviation from linearity was observed. Mass balance during photooxidation was confirmed by determining the amount of NO_3^- product residues onto the photocatalyst surface.

© 2013 Elsevier B.V. All rights reserved.

1. Introduction

The development of economical and sustainable environmentally friendly treatment technologies to remediate hazardous air pollutants, especially in urban areas to levels that comply with strict legislation rules [1], poses one of the most critical challenges at the global scale. Among the targeted air pollution sources, emissions of nitrogen oxides (NO_x) have received great attention on account of their serious environmental and health effects. Heterogeneous photocatalytic oxidation (PCO) using titanium dioxide (TiO_2), employed either in nanoparticulate [2] or nanotubular morphology [3], has emerged as a highly promising remediation technology for the reduction of NO_x emissions owing to the significant advantages that this method offers over conventional ones [4–7]. PCO of NO molecules adsorbed on the TiO_2 surface takes place with either hydroxyl ($^{\bullet}OH$) or superoxide radicals ($O_2^{\bullet-}$), formed after photoexcitation of the material. In the first route, photogenerated holes in the TiO_2 valence band react with adsorbed water molecules or/and OH^- anions at the semiconductor/air interface, thus producing highly oxidative hydroxyl radicals ($^{\bullet}OH$). The ($^{\bullet}OH$) reaction with NO proceeds via the formation of unstable nitrous acid and NO_2 and completes with the formation of HNO_3 as the major photo-oxidation product deposited on the catalyst [8–10]. Alternatively, PCO can proceed via $O_2^{\bullet-}$ radicals produced by O_2 reaction with the photogenerated TiO_2 conduction band electrons that can either directly react with NO_x or indirectly via other formed reactive species like peroxide radicals ($^{\bullet}OOH$) and singlet oxygen $^1O_2$ [11–14]. The O_2 reduction pathway is considered to play a vital role in visible light photocatalysis since the holes trapped at the N-induced midgap level of N-TiO_2 may not have the required oxidation potential to produce hydroxyl radicals [12,14].

Nanoparticulate TiO_2 presents unique photocatalytic reactivity stemming from its high surface area and adsorption capacity [4]. In most cases, TiO_2 nanomaterials are immobilized on different types of substrates, including glass plates, glass rings, fibers, silica, polymer, zeolite, and alumina [15–18] in order to avoid additional filtration steps, whereas the photocatalytic oxidation of various gas pollutants is achieved utilizing continuous-flow or batch photocatalytic reactors [19–21]. However, one of the major drawbacks that limits the widespread technological application of TiO_2 photocatalysis stems from its wide bandgap (3 eV for the rutile phase and

* Corresponding authors. Tel.: +1 302106503644; fax: +1 30210651766.
E-mail addresses: akontos@chem.demokritos.gr (A.G. Kontos), papi@chem.demokritos.gr (P. Falaras).

0926-3373/$ – see front matter © 2013 Elsevier B.V. All rights reserved.
http://dx.doi.org/10.1016/j.apcatb.2013.04.070

3.2 eV for the anatase phase). This inherent limitation of TiO_2 photocatalysts requires the application of ultraviolet irradiation for the activation of the photocatalytic procedure, while the abundant visible light radiation of the solar spectrum or of any other artificial light source remains unutilized.

Consequently, extensive research efforts have been devoted to the development of modified photocatalytic materials, whose photoresponse can be broadened and shifted in the visible light spectrum, mainly via doping TiO_2 with anions such as nitrogen, carbon, sulfur, and halides [4,22–25]. Among these species, nitrogen has been the most efficient dopant enabling the photocatalytic degradation of aqueous organic [26–30] and gaseous pollutants [31,32]. N-TiO_2 visible light photocatalysts prepared by chemical (treatment with hexamethylenetetramine [33,34]) or physical methods (annealing in NH_3 atmosphere [11]), were also proved to be very effective in the photocatalytic oxidation of NO_x.

Co-doping of TiO_2 with nitrogen and fluorine (NF-TiO_2) appears as a promising modification route that improves the structural stability of titania, while attaining a high visible light photocatalytic activity towards noxious organic pollutants due to synergistic effects between the N and F dopants [35–37]. Fluorine doping inhibits the phase transformation from anatase to rutile as well as the removal of N-dopants during thermal annealing [38]. Furthermore, N-F co-doping has been predicted to reduce oxygen defects in the TiO_2 lattice, by charge compensation between the nitrogen (p-type) and the fluorine (n-type) dopants [39]. These effects stabilize the composite system and effectively reduce the concomitant electron-hole recombination that deteriorates the visible light induced photocatalytic efficiency of single doped N-TiO_2. NF-TiO_2 prepared by the sol gel method in the presence of ammonium fluoride [40] was investigated in the mineralization of acetic acid in aqueous suspensions and acetaldehyde in the gas phase showing improved performance relative to reference compounds (e.g., P25). Furthermore, action spectra (photocatalytic decomposition as a function of the wavelength from 370 to 460 nm) were reported and compared to the absorbance spectra in the same range. Recently, we have further exploited NF-TiO_2 doping by employing a modified sol gel technique based on a nitrogen precursor and a nonionic fluorosurfactant, as both fluorine source and pore template material to tailor-design the TiO_2 structural properties. This photocatalyst exhibited significant photocatalytic degradation efficiency against cyanotoxin pollutants in water both in slurry [41] and immobilized forms [42] as well as enhanced photoinduced hydrophilicity under visible light illumination [43].

The present study aims at presenting a new and innovative path in the area of NO gas pollutant photodecomposition under daylight illumination by using NF-TiO_2 films and employing a single-pass, open-flow reactor (continuous-flow) apparatus. The kinetics of the photocatalytic reaction was investigated with respect to the pollutant initial concentration (200–800 ppbv) and the intensity of the absorbed light irradiance. This permitted direct comparison of PCO with UV and daylight excitation and determined a range where the PCO rate depends linear on the light irradiance. Nitrogen mass balance during the PCO reaction, scarcely addressed up to now in the literature of visible light active photocatalysts, was also studied.

2. Experimental

2.1. Preparation and characterization of the N-F-doped TiO_2 nanocrystalline films

NF-TiO_2 films were prepared by the surfactant assisted sol gel method according to [41–43] by employing ethylenediamine as a nitrogen precursor and Zonyl FS-300 nonionic fluorosurfactant as fluorine precursor and pore template. Photocatalysts were immobilized on borosilicate glass by dipping the substrate in and pulling it out from the sol at a withdrawal rate of 12.5 ± 0.3 cm min^{-1}. Deposition was followed by calcination at 400 °C for 30 min in air, in order to enhance TiO_2 crystallization. The dip-coating and calcination cycle was repeated for 3-times, and the coatings reached a thickness of approximately 1.9 μm. Such films covering an area $A = 39.5$ cm^2 were used for the photocatalytic experiments.

Table 1
Light Irradiance (I) on the photocatalyst surface and corresponding absorbed irradiance by the films (I_{abs}) as a function of the light source and the number of irradiating lamps.

No of lamps	Daylight I (W m^{-2})	I_{abs} (W m^{-2})	UV I (W m^{-2})	I_{abs} (W m^{-2})
1	1.0	0.11	0.35	0.25
2	2.0	0.22	0.74	0.53
10	7.6	0.86	2.60	1.87

The NF-TiO_2 films were thoroughly characterized for their physicochemical properties in the past [41–43]. Some characterizations, like micro-Raman spectroscopy and UV–vis spectroscopy, were repeated giving identical results. In addition, the film morphology was characterized by high magnification scanning electron microscopy (SEM) using a PHILIPS Quanta Inspect microscope and atomic force microscopy (AFM) with a digital Instruments Nanoscope III microscope, operating in the tapping mode.

2.2. Photocatalytic system characteristics

Photocatalytic oxidation experiments were carried out by employing a recently developed continuous-flow photocatalytic system [3], schematically shown in Fig. 1, comprised of the gas delivery unit, the continuous-flow photocatalytic reactor equipped with the appropriate light source, and the acquisition unit. The design and operation of the system were adapted from the ISO 22197-1: 2007 international standard [44]. The reactor chamber was a glassy cube with a 0.001 m^3 total volume capacity. The chamber was placed inside a light sealed irradiation box, constructed with stainless steel. Illumination was provided by ten lamps placed horizontally in pairs on each side of the irradiation box at a distance of approximately ~20 cm from the NF-TiO_2 photocatalytic film. Each lamp (length: 45 cm and diameter: 28 mm) is equipped by a switch, allowing independent use. Philips FSL-15 W lamps were used for providing daylight illumination, whereas Philips TLD-15 W fluorescent black light blue lamps were used for ultraviolet irradiation. The spectral distributions of the lamps are shown in Fig. S1 (supplementary material), in comparison with the absorbance spectrum of the NF-TiO_2. Irradiance at the photocatalytic surface was measured by a 28-0925 Ealing Research radiometer, taking into consideration its spectral calibration factor. Values of irradiance by using 1, 2 and 10 lamps of either light source are given in Table 1, showing that daylight was more intense than UV. However, the films are very poor absorbers of the visible light. Thus absorbed irradiance by the films was calculated as $I_{abs} = \int I_i(\lambda)\, A(\lambda)\, d\lambda$, where $I_i(\lambda)$ and $A(\lambda)$ are the spectral responses of the incident $I_i(\lambda)$ irradiation and the absorbance of the films, obtained by the corresponding profiles in Fig. S1, in accordance to [43]. Yielded I_{abs} values are presented in Table 1 and were a fraction of 72% of the UV and only 11% of the daylight incident irradiances.

The ability of the N-F-doped material to decompose NO was tested for four different NO concentrations and specifically for $C_{NO} = 200$, 400, 600, and 800 ppbv. In order to achieve the desired initial NO concentration in the reaction chamber, NO rich gas, provided by a compressed gas cylinder of 10 ppmv NO (±2%) balanced in N_2, was mixed with the appropriate

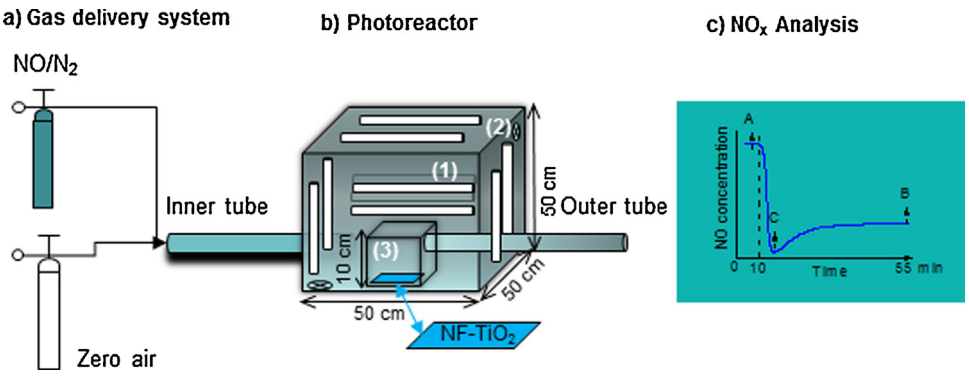

Fig. 1. Schematic representation of the continuous flow photocatalytic reactor with 10 lamps on the surrounding walls (1) and two fans (2) for stabilizing room temperature conditions. A 1 dm^3 cubic Pyrex glass cell (3) was placed in the center of the ground face of the chamber carrying the NF-TiO_2 films at the bottom. NO pollutant was fed through the inlet pipe and NO_x was sampled at the outlet. The inset graph presents schematically the typical form of the NO photocatalytic oxidation kinetics.

quantity of synthetic air (20.5% v/v O_2 and 79.5% v/v/N_2) prior to its introduction to the chamber. Calibrated flow meters were used to adjust and control the gas flow rate at 2–2.5 L/min. These, moderate rates were chosen in order to minimize mass transfer limitation phenomena above the material's surface [45]. The concentration of NO at the outlet of the reactor chamber was measured with a Chemiluminescence NO_x analyzer (Model 42c, Thermo Environmental Instruments Inc.), providing instant records of the NO, NO_2 and NO_x concentrations. Experiments were performed under ambient temperature (24–27 °C) and humidity (35–45%) levels (continuously measured with a thermo-hygrometer) secured by the constant operation of two fans inside the environmental box with the ultimate purpose to evaluate the performance of the materials in real conditions and hence assess the possibility of incorporating them into future environmental applications.

2.3. Photocatalytic experimental procedure

Prior to photocatalysis, the NO–air mixture was driven through the by-pass line directly to the NO_x analyzer in order to set the desired value of the initial pollutant concentration and check the response of the measurement system. Subsequently, the air mixture was channeled to the reaction chamber. Data acquisition began and the system was left to equilibrate for 30 min. After the stabilization of the pollutant's concentration (point A of the schematic kinetic graph in Fig. 1c), the lamps were switched on and the NO_x concentration was constantly recorded with respect to the reaction time for at least 45 min, up to the point of the NO equilibrium (point B in Fig. 1c). Steady state of PCO is gradually reached via a transient initial abrupt response of the system where a strong decrease of the NO concentration is observed right after switching on the irradiation lamps (point C in Fig. 1c). After completing the experiment, the lamps were turned off and the system was allowed to re-equilibrate to the non irradiated condition. Then, a last measurement was taken to confirm the initially measured NO concentration level.

Mineralization residues on the photocatalyst surface were examined with ion chromatography after performing long lasting (2 h) photocatalytic experiments under maximum irradiation intensity provided by 10 daylight lamps and by adjusting the initial NO concentration in the reaction chamber to a high value (1000 ppb) and the gas flow rate to 1.7 L/min. After completion of the photocatalytic treatment, the NF-TiO_2 films were rinsed with 80 ml deionized water and ion analysis of the aqueous solutions was performed in a Dionex ICS-1100 RFIC ion Chromatographer employing an IonPac AC22 anion-exchange column.

3. Results and discussion

3.1. Film properties–surface characterization

The NF-TiO_2 films exhibit enhanced structural properties, i.e. high surface area (136 m^2/g), high porosity (48%) and a mesoporous structure with a narrow pore size distribution (2–10 nm). The amount of TiO_2 deposited upon each dip coating layer deposition was $W_1 = 160\ \mu g\ cm^{-2}$ [42]. As the number of performed coating cycles (3) and the area of the films (A), a total film weight of $W = 3\ A\ W_1 = 19$ mg was attained. X-ray photoelectron spectroscopic analysis revealed that nitrogen and fluorine atoms are introduced in the TiO_2 lattice with atomic concentrations of 1.5 and 4.9%, respectively. Anatase was identified as the major TiO_2 polymorphic phase and brookite as a secondary, while the optical absorption extends up to 510 nm (2.43 eV) [43]. Electron paramagnetic resonance spectroscopy has shown the presence of N spin species with a high sensitivity to the visible light irradiation that supports synergistic effects between fluorine and nitrogen dopants. Further, surface characterization of the NF-TiO_2 films by scanning electron and atomic force microscopies (see Fig. S2 in the supplementary material) has shown that the films present a macro porous regular morphology with circular craters having diameters between 5 to 8 μm and depth of about 400 nm. This morphology provides a large scale roughness component without deteriorating the adherence of the films on the substrate. This can be considered as a beneficial feature of the sol–gel films since it increases the effective surface area of the catalyst and promotes surface wetting and pollutant adsorption.

3.2. Photocatalytic activity under maximum irradiation of the films (10 lamps)

On account that the total reduction in the amount of NO during the photocatalytic process also comprises the amount of NO that is removed due to adsorption of the air pollutant on the cell walls and/or radiation photolysis, blank tests similar to those commonly applied in the literature [4,6,8], were initially performed. In these experiments, the air mixture was introduced in the chamber and was irradiated in the absence of the photocatalyst. The displayed concentration of NO in the gaseous NO–zero air mixture remained stable over the whole 45 min experimental period. This result indicated that either variations attributed to these background phenomena are negligible or their duration was quite short and equilibrium to the initial value was quickly reached.

Then, photocatalytic experiments were conducted by inserting the catalytic films inside the reaction chamber under maximum illumination intensity using all the light sources (10 lamps) in order

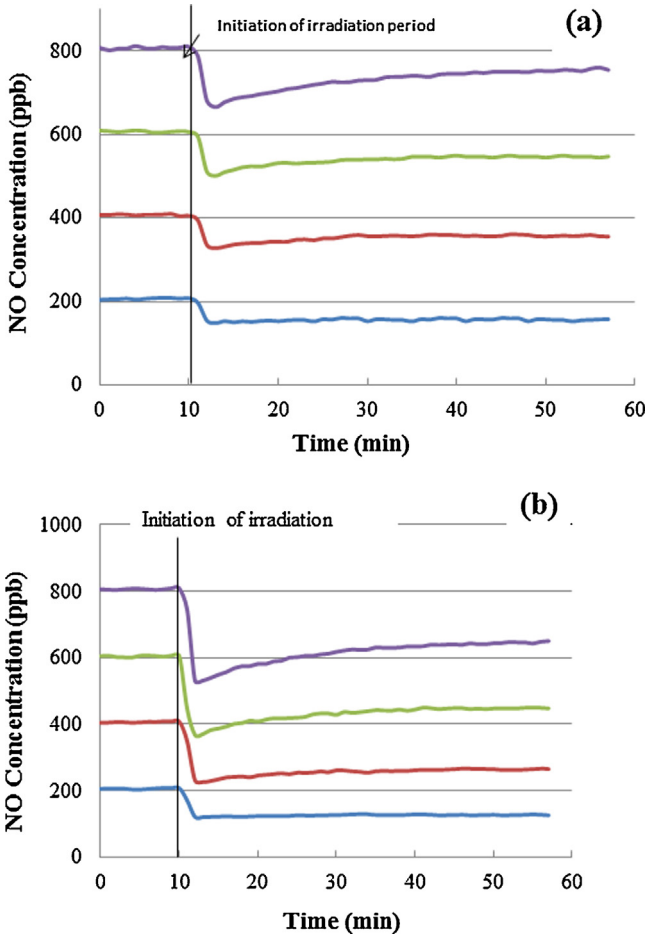

Fig. 2. NO concentration vs. irradiation time under daylight (a) and UV (b) irradiation of the NF-TiO_2 thin film photocatalysts.

to obtain the highest photocatalytically oxidized NO amount. The obtained NO kinetics for different NO initial concentrations are summarized in Fig. 2, revealing that the N-F-doped films were highly active in the degradation of NO. Right after the initiation of the irradiation period, the initial concentration of NO rapidly dropped to a minimum value, where it remained for a short time, and then slowly increased reaching a steady state at the outlet, in accordance to the literature [3,6,8,10,46]. Apart from NO, traces of NO_2 formed gas was also detected in the outlet. Typical NO_2 concentration profiles, together with corresponding NO and NO_x profiles under daylight illumination are presented in Fig. S3 (supplementary material). Nevertheless, in all cases, the concentration ratio of NO_2 vs. NO was less than 3% and near to the detection limit of our system. This very low NO_2 selectivity is normal in experiments where the concentration level of the inlet NO gas is in the ppb level [3,10]. Accumulated NO_2 photocatalytic product became significant at high NO inlet concentration levels and long acquisition experiments (see Section 3.5)

The ability of the NF-TiO_2 to decompose NO was evaluated after the system reached steady state conditions, through the calculation of two parameters, the percentage of NO removal, η (%), given by Eq. (1) and the photocatalytic oxidation rate (r) defined by Eq. (2) [2,3].

$$\eta(\%) = \left[\frac{(C_{in} - C_{out})}{C_{in}}\right] 100 \quad (1)$$

$$r(\mathrm{mg/m^2 s}) = (C_{in} - C_{out})F/A \quad (2)$$

Table 2
Percentage of NO removal (η) and photocatalytic oxidation rate (r) for various initial NO concentrations by illuminating NF-TiO_2 films under daylight and UV with maximum irradiance.

NO concentration	200 ppb	400 ppb	600 ppb	800 ppb
η_{vis} (%)	24.2	12.2	9.9	6.7
η_{UV} (%)	38.6	35.0	25.9	20.1
r_{vis} ($\mu g\,m^{-2}\,s^{-1}$)	0.55	0.54	0.66	0.57
r_{UV} ($\mu g\,m^{-2}\,s^{-1}$)	0.86	1.50	1.61	1.76

where, F (m^3/s) is the flow rate, A (m^2) is the illuminated photocatalyst area and C_{in}, C_{out} ($\mu g/m^3$) are the inlet and outlet NO concentrations, respectively. C_{in} was determined by the equilibrium value of the NO concentration that was recorded over a 10 min period before the lamps were switched on, while C_{out} by the corresponding value recorded at the end of irradiation period (which lasted for 45 min).

The computed photocatalytic parameters η and r, shown in Table 2, present markedly different dependence on the pollutant concentration and the irradiation source. The highest photocatalytic oxidation efficiency that was achieved under daylight illumination was $\eta = 24.2\%$ (Table 2) and was attained with the minimum pollutant concentration (200 ppb). This η value is comparable to that observed under similar experimental conditions for carbon doped TiO_2 [46] despite they used much higher film surface area (167 cm^2). Also it is slightly lower than the value of 27% obtained for N-TiO_2 [11], even though they used diodes for illuminating the samples at 445 nm, where the photocatalyst strongly absorbs. Furthermore, the photocatalytic oxidation rate saturated to about 0.66 $\mu g\,m^{-2}\,s^{-1}$ (The r values for C_{in} 600 and 800 ppb are quite similar), posing an upper threshold for the amount of NO that can be photocatalytically oxidized under the applied experimental conditions (daylight illumination at 7.6 $W\,m^{-2}$, gas flow rate of 2–2.5 L/min and limited exposed coated area of the catalyst). On the contrary, the effect of the pollutant concentration level on the material's performance was less prominent under UV radiation, indicative of faster photocatalytic kinetics relative to those under daylight illumination. In fact, the obtained results under UV (Table 2) showed that the NF-TiO_2 films maintain a sufficiently high photocatalytic performance even at high initial concentrations ($\eta > 20.1\%$) and present a continuous increase of the photocatalytic oxidation rate up to 1.76 $\mu g\,m^{-2}\,s^{-1}$ upon increasing the pollutant concentration to 800 ppb, in general agreement with the literature [47].

Furthermore the PCO rates of nitrogen oxide by the NF-TiO_2 films under UV, daylight and visible (daylight lamps with 400 nm cutoff filter) illumination were compared with the corresponding rates obtained by reference photocatalytic films using the benchmark photocatalyst Evonik P25 [48], under the same experimental conditions. The results are summarized in Fig. S4 in the supplementary material. Considerable photocatalytic oxidation of NO gas pollutant takes place using the NF-TiO_2 films under pure visible light illumination (use of a 400 nm cut-off filter), where Evonik P25 is completely inactive. However, the efficiency of Evonik P25 films is higher under daylight illumination conditions. This can be attributed to its rutile component (which extends the aborbance up to 400 nm) and its optimized thickness (5–5.5 μm) for maximum light absorption. It is worth noting that the NF-TiO_2 films perform slightly better than P25, under UV irradiation, which can be attributed to its higher BET surface area [42]. These results are in very good agreement with literature data of doped TiO_2 [40], where it was observed that UV light has very high photoactivity (while visible light has very low), despite the inference of the corresponding action spectra.

Concerning the N-doped-TiO_2 visible photocatalysis, a possible mechanism involves the O_2 reduction pathway and was discussed

in the introduction [11–14]. In addition, recently, Barolo et al. [49] proposed a 'slow' two-step excitation process for the generation of surface charge carriers in N-TiO_2. In this mechanism, visible light excites electrons from the nitrogen isolated mid-gap states (lying a few meV over the limit of the valence band) to the semiconductor conduction band whereas these states receive electrons from the valence band via excitation in the NIR range. Both the above mechanisms are consistent with the relatively low efficiency of the N-F doped photocatalysts in the visible region (with respect to the effect of UV radiation) [40–42] and justify well the experimental results of the present work.

3.3. Effect of the light irradiance on the photocatalytic performance of the material

The effect of the incident light irradiation was subsequently investigated by repeating the photocatalytic experiments using only 1 or 2 lamps in the photocatalytic chamber. The effect of the UV light intensity on the PCO reaction rate has been clearly demonstrated in the literature of photocatalysis [10,46,47,50,51]. Theoretical and experimental studies have shown that the photocatalytic reaction occurs in two regimes in association with the irradiance of UV light (I). For low photon flux, the degradation increases proportional to I (first order regime), whereas at high photon flux the photocatalytic activity grows with the square root of I (half order regime) [50,51]. The transition from the first to the half order regime occurs when I approaches the solar irradiance, ($I = 1000\,W/m^2$ for 1 sun, whereas the UV component is of the order of $50\,W/m^2$), however this is uncertain for low pollutant concentration [10]. Despite the thorough investigations on the effect of the ultraviolet radiation intensity on the photocatalytic reaction rate, the corresponding effect of daylight irradiation has been rarely addressed, apart from a recent work [46], where the NO_x conversion rate was reported to increase with the increase of I from 1.0 to $13.0\,W/m^2$, following a logarithmic law.

In order to give insight into the above dependence, irrespectively of the light source, the overall NO reaction rates were plotted against the absorbed daylight irradiance in Fig. 3a. A linear relationship of the form $r = r' I_{abs}$ (r' is a coefficient, independent of flux, relating r with I_{abs}) was thus derived under daylight illumination within the NO concentration regime of 200–800 ppb, consistent with the first order regime of the photocatalytic degradation rate dependence on the irradiance.

A similar plot of the NO photocatalytic oxidation rates against the absorbed irradiance has been constructed for the UV irradiation in Fig. 3b. For maximum UV irradiation (10 lamps), the photocatalytic oxidation rates tend asymptotically to a plateau, most clearly observed for the lowest 200 ppb NO concentration level, that indicates mass-transferred controlled kinetics [51]. By fitting the data to a power law of the form $r = r' I_{abs}^{b}$, a constant $b = 0.55 \pm 0.13$ is found for all concentrations in between 200 and 800 ppb, which shows that the system tends to obtain the square root dependence, characteristic of the half order regime. The threshold of the transition from the first to half order regime was accordingly found to shift from tens to only a few $W\,m^{-2}$, due to the ppb NO concentration level [10]. It is also remarkable that by constructing the plots based on the absorbed light irradiance by the NF-TiO_2 films, the obtained reaction rates under UV and daylight irradiation become quite similar.

3.4. Investigation of the influence of the NO concentration on the initial reaction rate

Analysis of the transient photocatalytic oxidation kinetics in Fig. 2 permitted calculation of the initial reaction rate r_{in} which was estimated by the difference in the NO concentration before irradiation (C_{in}) and 5 min after irradiation of the photocatalyst (C_{irrad}) where a minimum in the pollutant concentration is reached and is given by Eq. (3), in analogy to Eq. (2):

$$r_{in} = \left[\frac{(C_{in} - C_{irrad})F}{A}\right] \quad (3)$$

Results on the dependence of the initial photooxidation rate on the pollutant concentration are shown in Fig. 4, for irradiation with 10 lamps. Up to the 800 ppb NO initial concentration, a linear dependence of the initial photooxidation rate on the NO concentration is observed. This behavior conforms with first order kinetics, in accordance to [46,52–54], and is justified by the continuous coverage of the material surface by NO molecules as far as the pollutant concentration increases. The initial rates observed in UV photocatalysis are 2–3 times higher than those attained with daylight photocatalysis. This difference also matches well the corresponding ratio of absorbed irradiance (see I_{abs} scales in Fig. 3 for daylight and UV light).

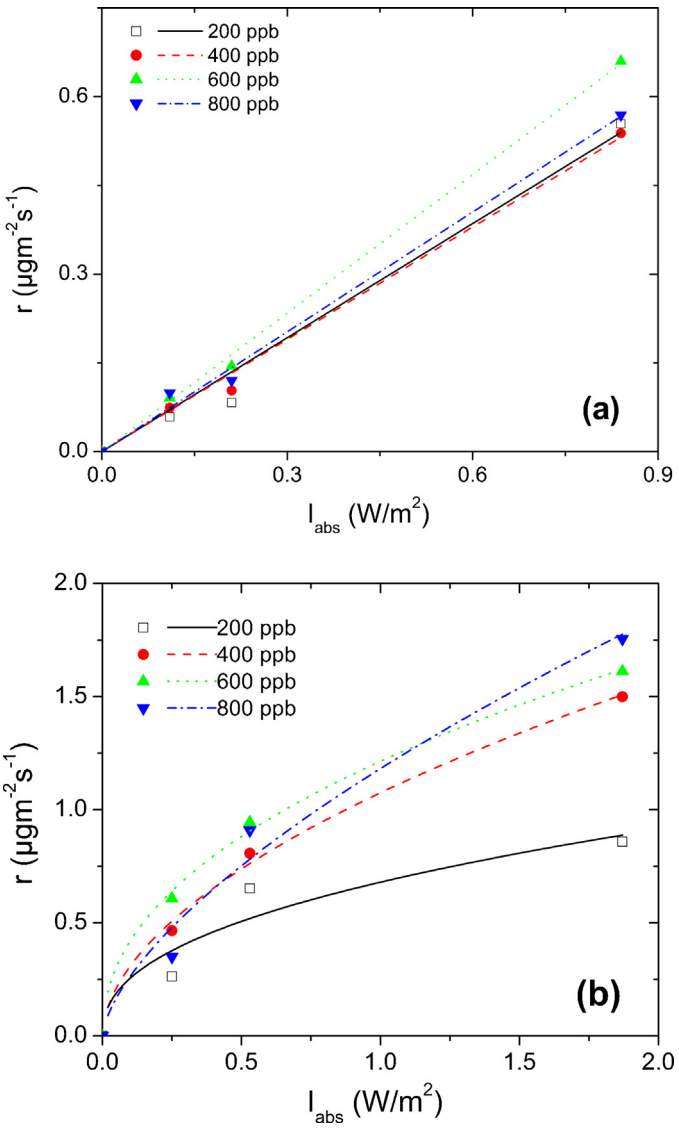

Fig. 3. Plots of the photocatalytic oxidation rates (r) vs. the absorbed irradiance (I_{abs}), for various initial NO concentration levels: data under daylight illumination with linear least square fitting (a) and under UV light irradiation with power law model fitting (b).

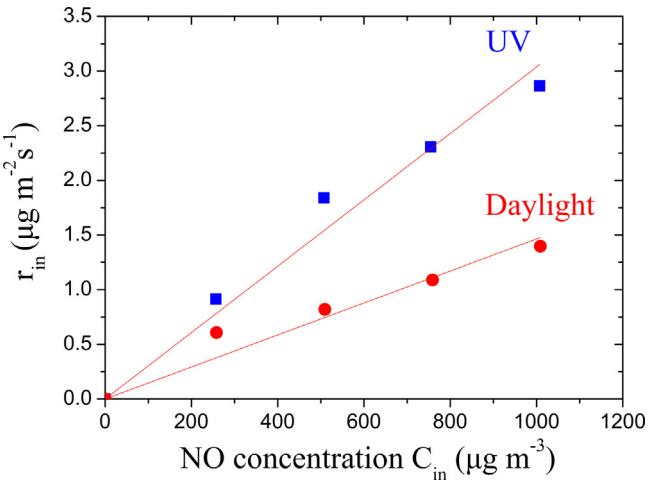

Fig. 4. Dependence of the initial photocatalytic oxidation rate (r_{in}) on the NO initial concentration (C_{in}), under daylight and UV light irradiation.

3.5. Identification of photocatalytic residues under daylight illumination

Formation and deposition of nitrate onto the surface of the NF-doped TiO_2 films was confirmed by ion chromatography after carrying out separate extended photocatalytic experiment by daylight illumination of the catalyst for 2 h (see the experimental part). To consider the nitrogen mass balance during the photocatalytic oxidation of NO on the films, the molar amount of NO transformed into NO_3 during the process ($\mathbf{Q}NO_{NO_3}$) was calculated by the difference of the molar amount of NO removed from air by daylight photocatalysis ($\mathbf{Q}NO_{vis\text{-}phot}$) and that transformed into NO_2 released in the gas phase ($\mathbf{Q}NO_{NO_2}$), according to the following relation [55]:

$$\mathbf{Q}NO_{NO_3} = \mathbf{Q}NO_{vis\text{-}phot} - \mathbf{Q}NO_{NO_2}$$

$$\text{where : } \mathbf{Q}NO_{vis\text{-}phot} = \frac{1}{MW_{NO}} \int_0^{120\ min} ([NO]_{in} - [NO(t)]_{vis})\, F dt$$

$$and\ \mathbf{Q}NO_{NO_2} = \frac{1}{MW_{NO_2}} \int_0^{120\ min} [NO_2(t)]_{vis} F dt \quad (4)$$

$[NO]_{in}$ is the concentration of NO in the inlet gas ($\mu g/m^3$), $[NO(t)]_{vis}$ and $[NO_2(t)]_{vis}$ are the time dependent concentrations of NO and NO_2 correspondingly in the outlet gas during daylight induced photocatalysis ($\mu g/m^3$), and F is the flow rate of the reaction gas ($m^3\ min^{-1}$). By calculating the above integrals from the NO_x profiles we obtained $\mathbf{Q}NO_{vis\text{-}phot} = 0.310\ \mu mol$ and $\mathbf{Q}NO_{NO_2} = 0.022\ \mu mol$. Their difference results in $\mathbf{Q}NO_{NO_3} = 0.288\ \mu mol$, from which, $mNO_3^-(calc) = 17.8\ \mu g$ of NO_3^- was calculated to be formulated onto the catalyst surface. This value is almost the same to that measured experimentally $mNO_3^-(meas) = 17.6\ \mu g$ by ion chromatography and verifies that the major photocatalytic product is HNO_3 in accordance to the literature findings in UV photocatalysis [10,55]. An amount of 0.288 μmol HNO_3 is thus accumulated in the surface of the 19 mg weighted photocatalytic film in the above experiment. According to [55], a film with such a weight can withstand a total HNO_3 amount of 0.76 μmol before its significant deactivation. In fact, after performing extended photocatalytic experiments (lasting about 10 h) without any intermediate cleaning of the films, the photocatalyst efficiency was reduced by approximately 50% due to fouling of the film surface by HNO_3 excess accumulating onto it.

4. Conclusions

This study reports on air cleaning environmental application of immobilized nitrogen and fluorine co-doped TiO_2 photocatalytic films under simulated natural light. A fluorosurfactant-based sol–gel method was employed to simultaneously achieve anion doping and improve the materials physicochemical properties. The NF-TiO_2 films were incorporated in a continuous flow reactor and examined for the photocatalytic oxidation of NO gas pollutants under daylight illumination. The reaction kinetics were studied over a wide range of NO concentrations (200–800 ppb) showing saturation of the photocatalytic oxidation (PCO) rate to about 0.66 $\mu g\ m^{-2}\ s^{-1}$ and maximum percentage of NO removal $\eta = 24.2\%$ obtained at 200 ppb. By increasing the irradiance from 1 to 7.6 mW/cm^2, a first order increase of the reaction rates was observed. Comparative evaluation of the materials performance under UV light irradiation showed a maximum η equal to 38.6% while the PCO rates reach a value of 1.76 $\mu g\ m^{-2}\ s^{-1}$ which is 2.7 times higher than the best value obtained under daylight illumination. A similar trend was observed in the transient kinetics. In general, difference of the PCO rates between UV and daylight illumination of the films is justified, in a large extend, by the much higher (2.2 times) net UV light absorbed irradiance by the films relative to the corresponding absorbed irradiance under daylight. Furthermore, in accordance with UV photocatalysis, nitrates were investigated as the principal photocatalytic residues by ion chromatography under daylight photoexcitation, too. This result is verified by the nitrogen mass balance analysis during the PCO process.

Acknowledgements

This research has been partially financed by the European Union (European Social Fund/ESF) and Greek national funds through the Operational Program "Education and Lifelong Learning" of the National Strategic Reference Framework (NSRF) – Research Funding Program: Thales-Investing in knowledge society through the European Social Fund/NANOMESO-MIS 377064. We wish to thank Ioannis Raptis for providing the spectral distribution of the lamps.

Appendix A. Supplementary data

Supplementary data associated with this article can be found, in the online version, at http://dx.doi.org/10.1016/j.apcatb.2013.04.070.

References

[1] EU-The Council of the European Union, Council Directive, 1999/30/EC-Relating to Limit Values for Sulphur Dioxide, Nitrogen Dioxide and Oxides of Nitrogen Particulate Matter and Lead in Ambient Air, 1999.
[2] T. Maggos, J.G. Bartzis, P. Leva, D. Kotzias, Applied Physics A 89 (2007) 81–84.
[3] A.G. Kontos, A. Katsanaki, V. Likodimos, T. Maggos, D. Kim, C. Vasilakos, D.D. Dionysiou, P. Schmuki, P. Falaras, Chemical Engineering Journal 179 (2012) 151–157.
[4] A. Fujishima, X. Zhang, D.A. Tryk, Surface Science Reports 63 (2008) 515–582.
[5] S. Kwon, M. Fan, A.T. Cooper, H. Yang, Critical Reviews in Environmental Science and Technology 38 (2008) 197–226.
[6] K. Hashimoto, K. Wasada, N. Toukai, H. Kominami, Y. Kera, Journal of Photochemistry and Photobiology A 136 (2000) 103–109.
[7] K. Hashimoto, H. Irie, A. Fujishima, AAPPS Bulletin 17 (2007) 12–28.
[8] A. Folli, S.B. Campbell, J.A. Anderson, D.E. Macphee, Journal of Photochemistry and Photobiology A 220 (2011) 85–93.
[9] D.F. Ollis, Comptes Rendus De L Acad. Sciences, Serie II Fascicule C-Chimie 3 (2000) 405–411.
[10] S. Devahasdin, C.J. Fan, K. Li, D.H. Chen, Journal of Photochemistry and Photobiology A 156 (2003) 161–170.
[11] S. Yin, B. Liu, P. Zhang, T. Morikawa, K. Yamanaka, T. Sato, Journal of Physical Chemistry C 112 (2008) 12425–12431.
[12] C. Cantau, T. Pigot, J-C. Dupin, S. Lacombe, Journal of Photochemistry and Photobiology A: Chemistry 216 (2010) 201–208.

[13] J.A. Rengifo-Herrera, K. Pierzchała, A. Sienkiewicz, L. Forro, J. Kiwi, J.E. Moser, C. Pulgarin, Journal of Physical Chemistry C 114 (2010) 2717–2723.
[14] R. Nakamura, T. Tanaka, Y. Nakato, Journal of Physical Chemistry B 108 (2004) 10617–10620.
[15] N.M. Takeda, S. Torimoto, S. Sampath, Journal of Physical Chemistry 99 (1995) 9986–9991.
[16] M.L. Sauer, D.F. Ollis, Journal of Catalysis 158 (1996) 570–582.
[17] M.E. Zorn, D.T. Tompkins, W.A. Zeltner, M.A. Anderson, Applied Catalysis B: Environmental 23 (1999) 1–8.
[18] M.E. Zorn, D.T. Tompkins, W.A. Zeltner, M.A. Anderson, Environmental Science and Technology 34 (2000) 5206–5210.
[19] M.M. Hossain, G.B. Raupp, S.O. Hay, T.N. Obee, AIChE Journal 45 (1999) 1309–1321.
[20] A. Bouzaza, C. Vallet, A. Laplanche, Journal of Photochemistry and Photobiology A: Chemistry 177 (2006) 212–217.
[21] S.B. Kim, H.T. Hwang, S.C. Hong, Chemosphere 48 (2002) 437–444.
[22] F. Han, V.S.R. Kambala, M. Srinivasan, D. Rajarathnam, R. Naidu, Applied Catalysis A-General 359 (2009) 25–40.
[23] S. Rehman, R. Ullah, A.M. Butt, N.D. Gohar, Journal of Hazardous Materials 170 (2009) 560–569.
[24] G. Liu, C. Han, M. Pelaez, D. Zhu, S. Liao, V. Likodimos, N. Ioannidis, A.G. Kontos, P. Falaras, P.S.M. Dunlop, J.A. Byrne, D.D. Dionysiou, Nanotechnology 23 (2012) 294003.
[25] C. Han, M. Pelaez, V. Likodimos, A.G. Kontos, P. Falaras, K. O'Shea, D.D. Dionysiou, Applied Catalysis B: Environmental 107 (2011) 77–87.
[26] Y. Izumi, T. Itoi, S. Peng, K. Oka, Y. Shibata, Journal of Physical Chemistry C 113 (2009) 6706–6718.
[27] J. Zhang, Y. Wu, M. Xing, S.A.K. Leghari, S. Sajjad, Energy & Environmental Science 3 (2010) 715–726.
[28] A.I. Kontos, A.G. Kontos, Y.S. Raptis, P. Falaras, Physica Status Solidi (RRL) 2 (2008) 83–85.
[29] H. Choi, E. Stathatos, D.D. Dionysiou, Applied Catalysis B 63 (2006) 60–67.
[30] H. Choi, M.G. Antoniou, M. Pelaez, A.A. Dela Cruz, J.A. Shoemaker, D.D. Dionysiou, Environmental Science and Technology 41 (2007) 7530–7535.
[31] Z.B. Wu, F. Dong, W.R. Zhao, S. Guo, Journal of Hazardous Materials 157 (2008) 57–63.
[32] J. Wang, H. Li, H. Li, S. Yin, S. Tsugio, Solid State Sciences 11 (2009) 182–188.
[33] S. Yin, H. Yamaki, M. Komatsu, Q. Zhang, J. Wang, Q. Tang, F. Saito, T. Sato, Journal of Materials Chemistry 13 (2003) 2996–3001.
[34] S. Yin, Y. Aita, M. Komatsu, J. Wang, Q. Tang, T. Sato, Journal of Materials Chemistry 15 (2005) 674–682.
[35] Y. Xie, Y. Li, X. Zhao, Journal of Molecular Catalysis A: Chemical 277 (2007) 119–126.
[36] S. Liu, J. Yu, W. Wang, Physical Chemistry Chemical Physics 12 (2010) 12308–12315.
[37] W. Wang, C. Lu, Y. Ni, M. Su, Z. Xu, Applied Catalysis B: Environmental 127 (2012) 28–35.
[38] G. Wu, J. Wen, S. Nigro, A. Chen, Nanotechnology 21 (2010) 085701.
[39] C. Di Valentin, E. Finazzi, G. Pacchioni, A. Selloni, S. Livraghi, A.M. Czoska, M.C. Paganini, E. Giamello, Chemistry of Materials 20 (2008) 3706–3714.
[40] M.V. Dozzi, B. Ohtani, E. Selli, Physical Chemistry Chemical Physics 13 (2011) 18217–18227.
[41] M. Pelaez, A.A. De la Cruz, E. Stathatos, P. Falaras, D.D. Dionysiou, Catalysis Today 144 (2009) 19–25.
[42] M. Pelaez, P. Falaras, V. Likodimos, A.G. Kontos, A.A. De la Cruz, K. O'Shea, D.D. Dionysiou, Applied Catalysis B: Environmental 99 (2010) 378–387.
[43] A.G. Kontos, M. Pelaez, V. Likodimos, N. Vaenas, D.D. Dionysiou, P. Falaras, Photochemical & Photobiological Sciences 10 (2011) 350–354.
[44] ISO. 22197-1: 2007- Fine ceramics (advanced ceramics, advanced technical ceramics) – Test method for air-purification performance of semiconducting photocatalytic materials – Part 1: Removal of nitric oxide.
[45] D. Chen, F. Li, A.K. Ray, AIChE Journal 46 (2000) 1034–1045.
[46] Q.L. Yu, H.J.H. Brouwers, Applied Catalysis B: Environmental 92 (2009) 454–461.
[47] R. Dillert, J. Stötzner, A. Engel, D.W. Bahnemann, Journal of Hazardous Materials 211–212 (2012) 240–246.
[48] A.G. Kontos, A.I. Kontos, D.S. Tsoukleris, V. Likodimos, J. Kunze, P. Schmuki, P. Falaras, Nanotechnology 20 (2009), 045603 (9pp).
[49] G. Barolo, S. Livraghi, M. Chiesa, M.C. Paganini, E. Giamello, Journal of Physical Chemistry C 116 (2012) 20887–20894.
[50] D.M. Blake, J. Webb, C. Turchi, K. Magrini, Solar Energy Materials and Solar Cells 24 (1991) 584–593.
[51] S.-K. Lee, A. Mills, Journal of Industrial and Engineering Chemistry 10 (2004) 173–187.
[52] D.D. Dionysiou, M.T. Suidan, I. Baudin, J.M. Laîné, T.L. Huang, Water Science and Technology 1 (2001) 139–147.
[53] V. Loddo, M. Addamo, V. Augugliaro, L. Palmisano, M. Schiavello, AIChE Journal 52 (2006) 2565–2574.
[54] P-A. Deveau, F. Arsac, P-X. Thivel, C. Ferronato, F. Delpech, J-M. Chovelon, P. Kaluzny, C. Monnet, Journal of Hazardous Materials 144 (2007) 692–697.
[55] Y. Ohko, Y. Nakamura, N. Negishi, S. Matsuzawa, K. Takeuchi, Journal of Photochemistry and Photobiology A: Chemistry 205 (2009) 28–33.